Pro-inflammatory effects of matrix metalloproteinase 7 in acute inflammation

RE Vandenbroucke[1,2], I Vanlaere[1,2], F Van Hauwermeiren[1,2], E Van Wonterghem[1,2], C Wilson[3] and C Libert[1,2]

Matrix metalloproteinase 7 (MMP7) is a member of the MMP family. In the small intestine, MMP7 is responsible for activating α-defensins, which are broad-spectrum anti-microbial peptides produced by the Paneth cells. We report that MMP7$^{-/-}$ mice are resistant to LPS-induced lethality and that this resistance is correlated with reduced levels of systemic cytokines. LPS induced the upregulation and activation of MMP7 in the small intestine, degranulation of the Paneth cells, and induction of intestinal permeability in MMP7$^{+/+}$ mice. In MMP7$^{-/-}$ mice, both LPS-induced intestinal permeability and consequent bacterial translocation to the mesenteric lymph nodes were reduced. Based on gene expression analysis and evaluation of intestinal damage, we attribute the protected state of MMP7$^{-/-}$ mice to reduced intestinal inflammation. Interestingly, we found that different α-defensins, namely Crp1 (DEFA1) and Crp4 (DEFA4), can stimulate IL-6 release in macrophages and ileum explants in a TLR4 independent way. We conclude that absence of MMP7 protects mice from LPS-induced intestinal permeability and lethality, and suggest that MMP7-activated α-defensins, in addition to their previously recognized bactericidal and anti-inflammatory roles, may exhibit pro-inflammatory activities in the intestine by activating macrophages and amplifying the local inflammatory response in the gut, leading to intestinal leakage and subsequent increase in systemic inflammation.

INTRODUCTION

Acute inflammation has an important role in the pathophysiology of systemic inflammatory response syndrome (SIRS), a lethal inflammatory disease caused by, e.g., trauma, burns, and infection. When infection is suspected, SIRS is called sepsis. Despite accumulating knowledge about SIRS and sepsis, current treatment is mainly limited to antibiotic treatment and support of vital functions. A better understanding of its pathology is therefore of extreme importance for finding new therapeutic targets.[1]

One of the major inflammation-provoking molecules is lipopolysaccharide (LPS), a component of the cell wall of Gram-negative bacteria, and, TNF, a major pro-inflammatory cytokine. These molecules induce considerable biological changes in many cell types. In recent years, it has become clear that the intestinal epithelial cells of the gut, which form an essential barrier between the lumen (which contains bacteria) and the sterile body, are particularly sensitive to inflammation.[2] Intestinal barrier dysfunction might lead to secondary bacterial translocation and multiple organ failure. This is lethal both in patients and in mouse models of sepsis and SIRS.[3–8]

The Paneth cells, present in the crypts of Lieberkühn of the small intestine, contribute to mucosal immunity by sensing bacteria and releasing anti-microbial peptides, such as α-defensins, which are also known as cryptdins (crypt defensins) and other proteins such as lysozyme C and phospholipase A2.[9] These molecules are active against a broad spectrum of pathogens, such as bacteria and fungi, and they enable the Paneth cells to create a microenvironment protected from infection and overgrowth of luminal bacteria, which assures continuous stem cell replication to maintain mucosal integrity.[10]

Mice express at least six anti-microbial α-defensins and numerous cryptdin-related peptides[11] depending on the particular mouse strain,[12] all of them having anti-microbial activities. In response to bacteria, Paneth cells release their secretory granules into the lumen of intestinal crypts.[9] Cryptdins are synthesized as procryptdins, which are activated by proteolytic cleavage. In mouse Paneth cells, the cleaving

[1]VIB Inflammation Research Center, Ghent, Belgium. [2]Department of Biomedical Molecular Biology, University Ghent, Ghent, Belgium and [3]Department of Pathology, University of Washington, Seattle, USA. Correspondence: C Libert (Claude.Libert@dmbr.vib-ugent.be)

Received 12 December 2012; revised 7 August 2013; accepted 25 August 2013; published online 16 October 2013. doi:10.1038/mi.2013.76

protease is MMP7, also known as Matrilysin. MMP7 is the smallest member of the family of matrix metalloproteinases (MMPs), which is composed of 25 zinc-dependent enzymes having roles in many physiological processes, such as embryo implantation, bone remodeling and organogenesis, as well as in many pathological processes.[13–15] Previously, we have shown that broad spectrum MMP inhibition protects mice against the lethal inflammation induced by injection of LPS.[16] The Paneth cells of MMP7$^{-/-}$ mice cannot release mature cryptdins and so these mice are hypersensitive to bacterial infections, such as *Salmonella typhimurium*[17] and *Chlamydia trachomatis*.[18] Intestinal MMP7 appears to be an essential molecule for mucosal protection but it has also been described as a mediator of inflammation in a mouse model of lung fibrosis and in DSS-induced colitis.[19,20] Recently, the latter was explained by the observation that MMP7-activated cryptdins can reduce the cellular release of IL-1β in DSS-induced colitis.[21] Here, we studied the role of MMP7 in acute, systemic inflammation by comparing the responses of wild-type and MMP7$^{-/-}$ mice to LPS-induced lethal inflammation.

RESULTS

MMP7$^{-/-}$ mice resist LPS-induced lethal inflammation

To investigate whether MMP7 has a role in acute inflammation, MMP7$^{+/+}$ and MMP7$^{-/-}$ mice were injected with LPS. LPS-induced systemic inflammation or endotoxemia is a well-accepted and validated model of SIRS characterized by pathological changes that strongly resemble sepsis.[22–24] As shown in **Figure 1a** all wild-type mice died but all MMP7$^{-/-}$ mice survived. This was also reflected in the body temperature

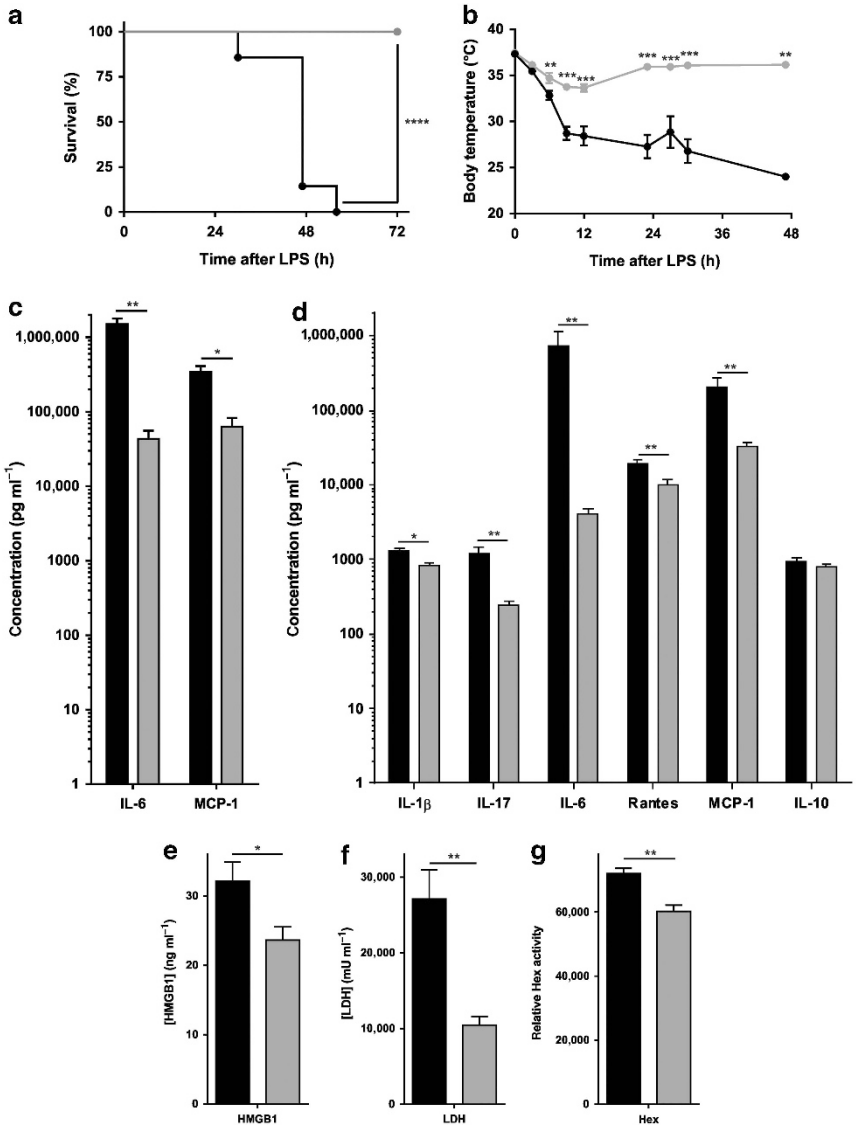

Figure 1 MMP7$^{-/-}$ mice resist LPS-induced lethal inflammation. (**a**) Survival and (**b**) body temperature of MMP7$^{+/+}$ (black; $n=7$) and MMP7$^{-/-}$ (gray; $n=8$) mice injected with 350 μg of LPS per 20 g body weight. Systemic cytokine and chemokine levels 4.5 h (**c**) and 9 h (**d**) after injection of LPS that are significantly different in MMP7$^{+/+}$ (black) and MMP7$^{-/-}$ (gray) mice ($n=5$). Plasma levels of (**e**) HMGB1, (**f**) lactate dehydrogenase (LDH), and (**g**) hexosaminidase (Hex) in LPS-injected MMP7$^{+/+}$ (black) and MMP7$^{-/-}$ (gray) mice 8 h after LPS injection ($n=4$–10) (*$0.01 \leqslant P < 0.05$; **$0.001 \leqslant P < 0.01$; ***$P < 0.001$).

of the mice (**Figure 1b**). At different time points after injection of LPS (0, 4.5, and 9 h), levels of serum cytokines and chemokines in wild-type and MMP7-deficient mice were measured. IL-6 and MCP-1 levels were significantly higher in MMP7$^{+/+}$ than in MMP7$^{-/-}$ serum samples both 4.5 and 9 h after LPS injection (**Figure 1c,d**). Also, IL-1β, IL-17, and Rantes were significantly higher but only at the 9 h time point (**Figure 1d**). No significant differences were observed for all the other cytokines (TNF, IL-1α, IL-2, IL-3, IL-4, IL-5, IL-9, IL-10, IL-12p40, IL-12p70, and IL-13) and chemokines (G-CSF, GM-CSF, IFNγ, KC, MIP1α, MIP1β, and eotaxin) that we measured (data not shown).

These results suggest that the acute inflammation is more intense in wild-type than in MMP7-deficient mice. In agreement with this, HMGB1, a relatively late marker of inflammation,[25] was also significantly higher in plasma of LPS-injected MMP7$^{+/+}$ mice (**Figure 1e**).

Similarly, after injection of LPS, plasma levels of lactate dehydrogenase and hexosaminidase, which are markers of general tissue damage[26] were higher in MMP7$^{+/+}$ mice than in MMP7$^{-/-}$ mice (**Figure 1f,g**). Our data provide strong indications that MMP7 has a detrimental role in acute, LPS-induced lethal inflammation.

MMP7 is expressed and activated in the Paneth cells of the ileum during endotoxemia

We analyzed MMP7 expression in different organs before and after systemic LPS injection by immunofluorescence and western blot. Lung, liver, kidney, and spleen analysis did not reveal MMP7 protein expression (**Supplementary Figures 1** and **2** online). mRNA expression analysis of the ileum showed an LPS-induced increase in *Mmp7* expression (**Figure 2a**). The MMP7 protein could be detected in the Paneth cells of the small intestine, in which MMP7 expression in secretory granules has been reported.[27] Immunofluorescent staining of ileum samples shows co-localization of MMP7 and lysozyme C, a well-validated Paneth-cell marker (**Figure 2b**). LPS challenge resulted in a decrease in MMP7-positive granules (**Figure 2c,d**), which suggests degranulation of the Paneth cells, which has been described before after stimulation with LPS and other TLR ligands.[28] In agreement with this, LPS injection resulted in a reduced number of toluidine blue-positive granules per crypt (**Figure 2e–g**) and analysis of the secretome of the ileum explants revealed an LPS-dependent increase in the Paneth cell-derived defensins (**Figure 2h**). Next, we measured MMP7 protein levels in flushed small intestines of LPS-injected mice by western blot analysis. Like all MMPs,

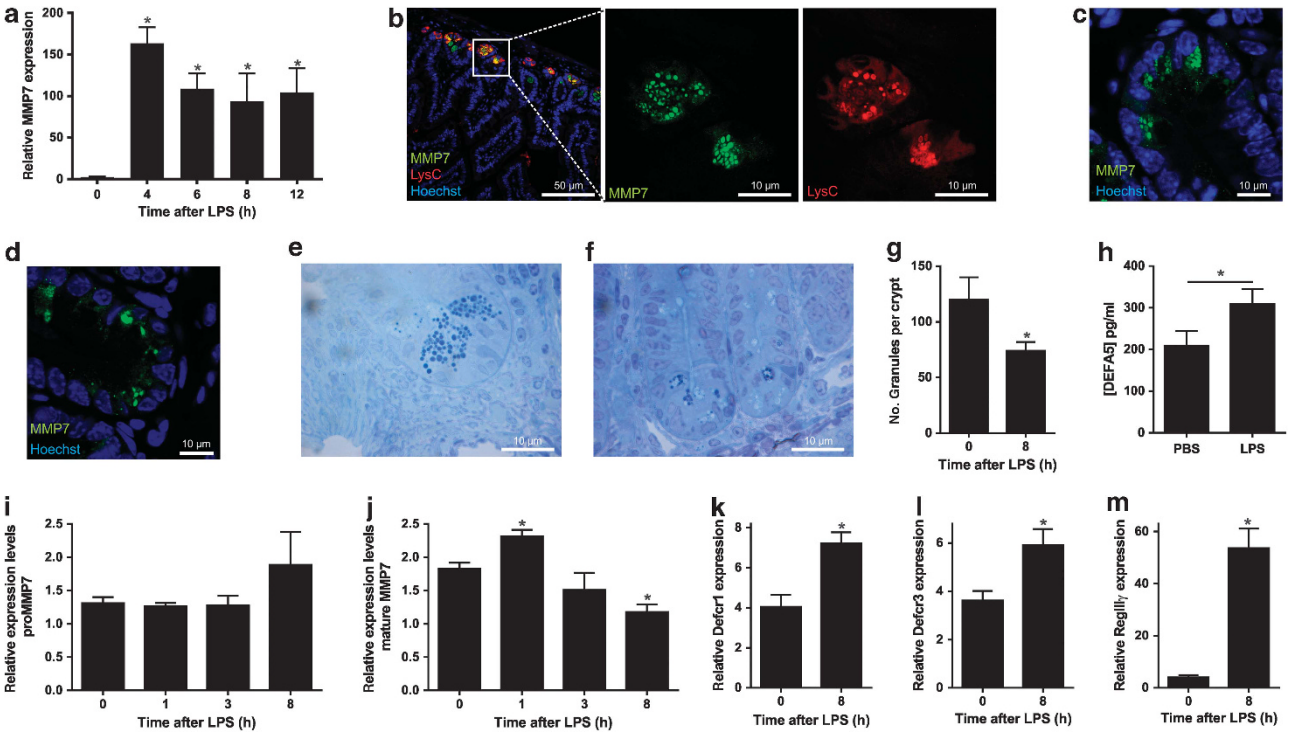

Figure 2 MMP7 expression and activation in Paneth cells of the ileum during endotoxemia. (**a**) Relative MMP7 mRNA expression in ileum 0, 1, 3, and 8 h after LPS injection ($n=4$-5). (**b**) Representative confocal image of ileum sections showing co-localization of MMP7 (green) and lysozyme C (red) in Paneth cells. Nuclei are stained with Hoechst (blue). (**c**,**d**) Representative confocal images of MMP7 in ileum before (**c**) and after (**d**) LPS stimulation. (**e**,**f**) Toluidine blue-stained ileum samples before (**e**) and after (**f**) injection of LPS. (**g**) Quantification of toluidine blue-stained granules per crypt in MMP7$^{+/+}$ mice before and after LPS challenge ($n=5$). (**h**) Quantification of DEFA5 levels secreted by *in vivo* LPS-stimulated ileum explants of MMP7$^{+/+}$ mice ($n=4$–6). (**i**,**j**) Quantification of proMMP7 (**i**) and mature MMP7 (**j**) in ileum lysates by western blot analysis 0, 1, 3, and 8 h after LPS ($n=3$–4). Normalization was done by comparison with β-actin levels. (**k–m**) Relative mRNA expression of Defcr1 (**k**), Defcr3 (**l**), and RegIIIγ (**m**) in total ileum lysates before and after LPS injection ($n=4$–6). Significance levels were calculated for differences from the corresponding 0 h time point and/or between MMP7$^{+/+}$ and MMP7$^{-/-}$ mice, as indicated (*$0.01 \leq P < 0.05$).

MMP7 is first produced as an inactive pro-form, which is activated by proteolytic cleavage. Wild-type mice were injected with LPS and pro- and mature MMP7 in ileum lysates were detected 0, 1, 3, and 8 h after LPS. Although proMMP7 remained constant until 3 h after LPS injection and showed a nonsignificant increase 8 h after LPS injection (**Figure 2i**), activated MMP7 first increased and then decreased (**Figure 2j**). These data illustrate that MMP7 activity is increased after LPS challenge and that this activated MMP7 is secreted into the lumen. This is in agreement with the results of *in vitro* experiments in which epithelial cells were exposed to bacteria.[29] Additionally, it is known that LPS exposure results in rapid and dose-dependent cryptdin secretion by the Paneth cells. Indeed, cryptdins *Defcr1* (*Defa1*) and *Defcr3* (*Defa3*), as well as *RegIIIγ* (*Reg3g*), were strongly upregulated after LPS injection, which suggests LPS-induced Paneth cell activation (**Figure 2k–m**). These data show that LPS results in increased MMP7 and cryptdins levels in the lumen after LPS challenge.

MMP7$^{-/-}$ mice are protected against LPS-induced gut permeability and bacterial invasion of the mesenteric lymph nodes

As LPS triggers expression and activation of MMP7 in the ileum crypts, and MMP7$^{-/-}$ mice are protected against LPS, we studied the mediator role of MMP7 in the small intestine during endotoxemia. We injected MMP7$^{+/+}$ and MMP7$^{-/-}$ mice with LPS and studied gut integrity by measuring the accumulation of orally administered FITC-dextran in the blood 0, 8, and 20 h after LPS injection. Gut permeability increased strongly in the MMP7$^{+/+}$ mice but much less so in MMP7$^{-/-}$ mice (**Figure 3a**).

To further address the importance of the gut barrier integrity in the endotoxemia model, we treated mice with epidermal growth factor (EGF), which has been shown to improve intestinal barrier function. Systemic administration of EGF limits intestinal tissue damage, thereby reducing mortality in different animal models of noninfectious and infectious inflammation and intestinal injury.[30–36] In our study, pretreatment of MMP7$^{+/+}$ mice with EGF reduced LPS-induced mortality (**Figure 3b**) and LPS-induced intestinal permeability (**Figure 3c**). Loss of gut barrier integrity can lead to efflux of bacterial gut flora or damage-associated molecular patterns, which can further activate inflammation by stimulation of PRRs in the submucosa, in the draining lymph nodes, or elsewhere.[37] To study this phenomenon in MMP7$^{+/+}$ and MMP7$^{-/-}$ mice, LPS was injected and bacterial translocation to the draining mesenteric lymph nodes (MLN) was quantified 24 h later. In agreement with the gut permeability results, we found a significant increase in bacterial presence in MMP7$^{+/+}$ but not in MMP7$^{-/-}$ MLN lysates after LPS challenge (**Figure 3d**).

To examine the role of intestinal bacteria in LPS-induced shock, we treated wild-type mice with antibiotics for 2 weeks to effectively eliminate bacteria from the gut, and then we injected sterile and non-sterile wild-type mice with LPS and monitored mortality. **Figure 3e** shows that sterile mice were protected against the lethal effects of LPS. Although germfree mice were shown to have reduced levels of MMP7,[29] we did not detect differences in *Mmp7* expression between the sterile and the non-sterile mice (**Figure 3f**), neither before nor after LPS administration. Moreover, we observed an additive effect of antibiotics treatment and MMP7 deficiency: intravenous injection of very high LPS doses (750 μg per 20 g body weight) resulted in 70% mortality of non-sterile MMP7$^{-/-}$ mice, whereas all sterile MMP7$^{-/-}$ mice survived (**Figure 3g**). Next, we analyzed the effect of antibiotics treatment on intestinal permeability. Unexpectedly, treatment of wild-type mice with antibiotics also protected against LPS-induced intestinal permeability. (**Figure 3h**). This result shows that intestinal bacteria have a role in amplification not only of systemic inflammation after leakage, but also of the local, intestinal inflammation preceding the leakage. In light of this, we had a closer look to the observation that α-defensins were shown to regulate the makeup of the commensal microbiota.[38] However, we could not detect any microbiome differences between MMP7$^{-/-}$ and MMP7$^{+/+}$ mice neither in feces nor in small intestinal content (data not shown). Additionally, the MMP7$^{-/-}$ mice show the same phenotype in a conventional facility, which indicates that limited changes in the microbiome do not affect the observed protection (data not shown).

Collectively, our data show that intestinal permeability and the presence of intestinal bacteria have important roles in the endotoxemia model. Additionally, these results suggest that MMP7 has a central role in the loss of gut barrier integrity and in the concomitant invasion of Gram-negative bacteria into the body. Increased gut permeability has been observed in multi-organ failure and in gastrointestinal disease[39,40] For example, in Crohn's disease, inflammation and loss of gut barrier integrity are associated with TNF as they are dramatically decreased by anti-TNF treatment.[41] As TNF injection has been reported to lead to loss of gut permeability,[42] it is interesting that MMP7$^{-/-}$ mice were also substantially protected against the TNF-induced lethal response (**Figure 3i**).

LPS-induced inflammation in the gut of MMP7$^{-/-}$ mice is less severe than that in MMP7$^{+/+}$ mice

Loss of gut integrity is typically a result of inflammation.[40] As MMP7$^{-/-}$ mice are protected against LPS-induced gut leakage, we studied whether LPS-induced inflammation in the small intestine is reduced in MMP7$^{-/-}$ mice. MMP7$^{+/+}$ and MMP7$^{-/-}$ mice were injected with LPS, and 0 and 8 h after challenge, the ileum was isolated and the innermost epithelial cells were harvested. qPCR analysis revealed an LPS-induced increase in the local expression of TNF (**Figure 4a**) and IL-6 (**Figure 4b**), two well-validated inflammatory molecules. Both TNF and IL-6 were induced to a significantly lower degree in the ileum of MMP7$^{-/-}$ mice compared with MMP7$^{+/+}$ mice, which indicates that the LPS-induced local inflammation in the small intestine is less pronounced in MMP7$^{-/-}$ mice. Besides TNF and IL-6, also the expression of iNOS (**Figure 4c**) was significantly lower in MMP7$^{-/-}$ mice than in MMP7$^{+/+}$ mice upon LPS challenge. In addition, based on previous results of our group and others, the lower systemic IL-17 levels in

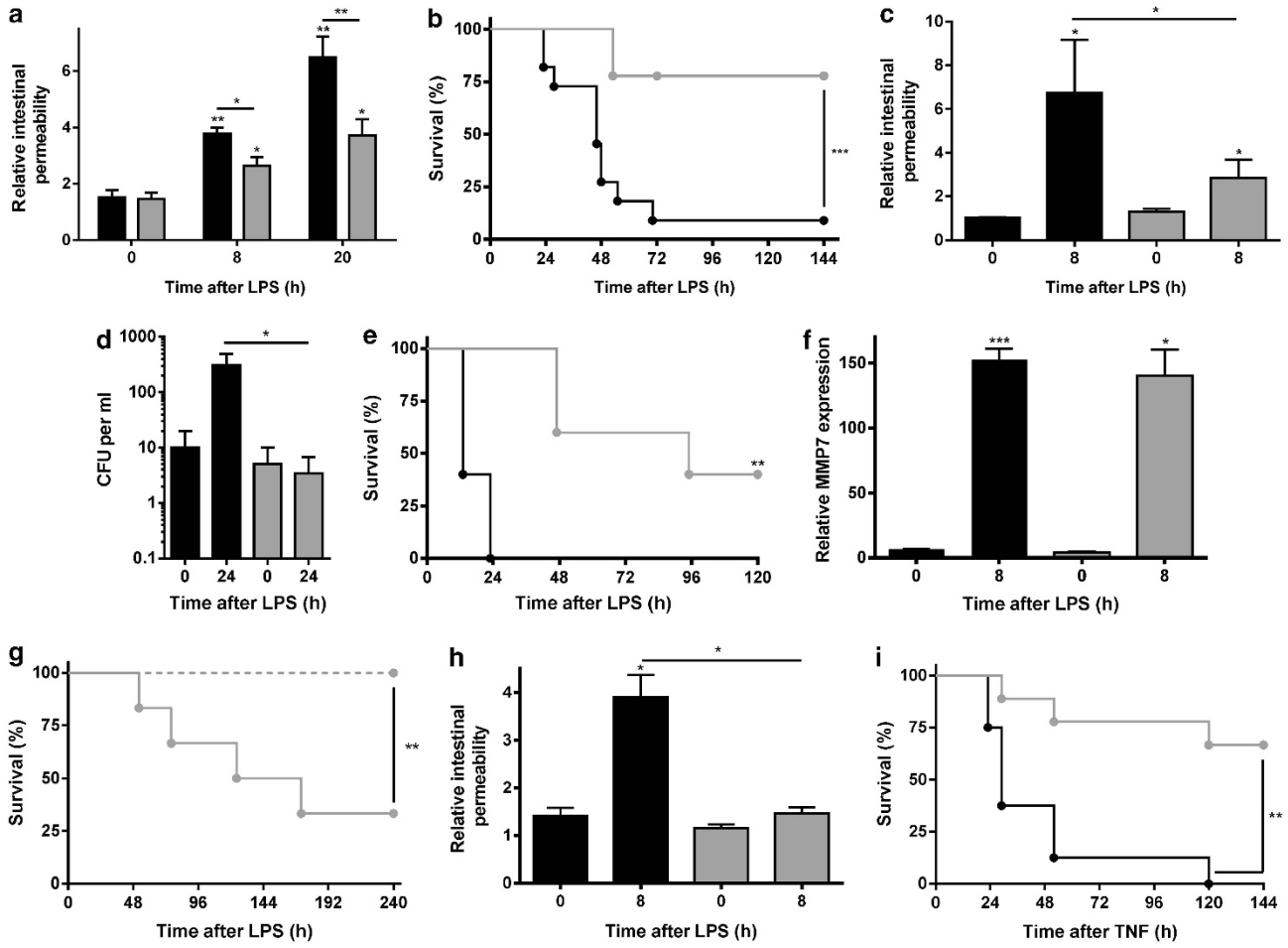

Figure 3 MMP7$^{-/-}$ mice are protected against LPS due to reduced LPS-induced gut permeability and bacterial invasion compared with MMP7$^{+/+}$ mice. (**a**) Relative intestinal permeability of MMP7$^{+/+}$ (black) and MMP7$^{-/-}$ (gray) mice before ($n=3$–4) and 8 h ($n=9$–11) and 20 h ($n=16$) after LPS injection ($n=10$–14). (**b**) Survival of MMP7$^{+/+}$ mice treated with PBS (black; $n=11$) or EGF (gray; $n=9$) 0, 6, and 9 h after LPS injection (350 μg per 20 g body weight). (**c**) Intestinal permeability of MMP7$^{+/+}$ mice before ($n=3$) and 8 h after LPS injection ($n=7$–8) treated 0, 3, and 6 h after LPS injection with PBS (black) or EGF (gray). (**d**) Bacterial load (CFU per ml) in MLN lysates of MMP7$^{+/+}$ (black) and MMP7$^{-/-}$ (gray) mice before and 24 h after LPS challenge. (**e**) Survival of non-sterile (black) and sterile (gray) MMP7$^{+/+}$ mice ($n=5$) injected with LPS (250 μg per 20 g body weight; intravenous(i.v.)). (**f**) MMP7 mRNA expression in sterile and non-sterile mice before ($n=3$) and after ($n=5$) LPS injection (250 μg per 20 g body weight; i.v.). (**g**) Survival of sterile (dotted gray; $n=8$) and non-sterile (gray; $n=6$) MMP7$^{-/-}$ mice injected with high LPS doses (750 μg per 20 g body weight; i.v.). (**h**) Relative intestinal permeability of non-sterile (black) and sterile (gray) MMP7$^{+/+}$ mice before ($n=3$) and 8 h after ($n=4$–5) LPS injection. (**i**) Survival of MMP7$^{+/+}$ (black; $n=8$) and MMP7$^{-/-}$ (gray; $n=9$) mice after TNF injection (30 μg per 20 g body weight). Significance levels were calculated for differences from the corresponding 0 h time point and/or between MMP7$^{+/+}$ and MMP7$^{-/-}$ mice, as indicated (*,$0.01 \le P < 0.05$; **,$0.001 \le P < 0.01$; ***,$P < 0.001$).

LPS-challenged MMP7$^{-/-}$ mice compared with MMP7$^{+/+}$ mice (**Figure 1d**) are also indicative for less intestinal inflammation.[43,44] The observed differences in inflammatory gene expression was not due to differences in white blood cell influx, as immunostaining showed equal amounts of CD45-positive cells in the ileum of LPS-treated MMP7$^{+/+}$ (**Figure 4d**) and MMP7$^{-/-}$ mice (**Figure 4e**). However, the observed reduction in LPS-induced inflammation was correlated with less intestinal damage (**Figure 4f**) and more mucin-containing goblet cells (**Figure 4g**) in MMP7$^{-/-}$ compared with MMP7$^{+/+}$ mice.

Cryptdins activate inflammation *in vitro* and *in vivo*

Although MMP7 has been shown to cleave many substrates *in vitro*, the main function of MMP7 in the small intestine might be the activation of these anti-microbial peptides, at least in mice. Small intestinal Paneth cells of the MMP7$^{-/-}$ mice cannot release mature cryptdins, which makes these mice hypersensitive to bacterial infections, such as *Salmonella typhimurium*[17] and *Chlamydia trachomatis*.[18] As we observed that MMP7-deficient mice are resistant to LPS-induced gut inflammation and to the consequent gut leakage and bacterial invasion, we hypothesized that MMP7-generated cryptdins might act as local amplifiers of inflammation. To test this, we incubated mouse macrophages with recombinant mouse Crp1 (DEFA1), Crp3 (DEFA3), and Crp4 (DEFA4), and measured IL-6 release in the supernatant. Both mouse Crp1 and Crp4 resulted in dose-dependent IL-6 secretion, showing that cryptdins have pro-inflammatory effects (**Figure 5a**). As none of the three cryptdins activated gene induction in a

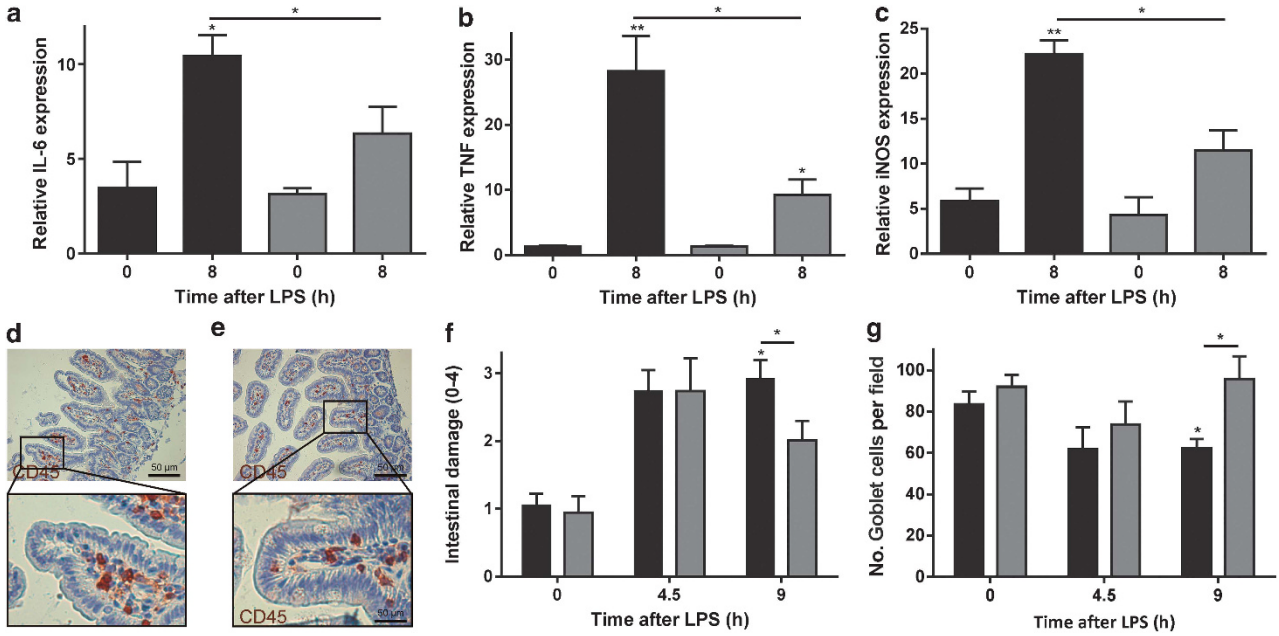

Figure 4 MMP7$^{-/-}$ mice show milder intestinal inflammation and are protected against LPS due to reduced LPS-induced gut permeability and diminished bacterial invasion compared with MMP7$^{+/+}$ mice. (**a**–**c**) Relative gene expression of IL-6 (**a**), TNF (**b**), and iNOS (**c**) in IEC-enriched ileum samples from MMP7$^{+/+}$ (black) and MMP7$^{-/-}$ (gray) mice before ($n=3$) and after LPS injection ($n=4$–5). (**d**,**e**) Representative images of CD45-stained ileum sections of LPS-treated MMP7$^{+/+}$ (**d**) and MMP7$^{-/-}$ (**e**) mice, 8 h after challenge. (**f**) Quantification of intestinal damage in MMP7$^{+/+}$ (black) and MMP7$^{-/-}$ (gray) mice before and 4.5 and 9 h after LPS injection, based on the evaluation of ileum sections stained with hematoxylin and eosin in a blinded setup by three neutral observers ($n=5$–6). LPS-induced intestinal damage is characterized by decreased villus height, disappearance of the mucus layer and goblet cells along the villus, cell death at the villus top, and cell debris in the lumen. (**g**) Quantification of mucin-containing Goblet cells in Alcian blue-stained ileum sections from MMP7$^{+/+}$ (black) and MMP7$^{-/-}$ (gray) mice ($n=5$–6), before and 9 h after LPS injection. Significance levels were calculated for differences from the corresponding 0 h time point and/or between MMP7$^{+/+}$ and MMP7$^{-/-}$ mice, as indicated (*$0.01 \leq P < 0.05$; **$0.001 \leq P < 0.01$).

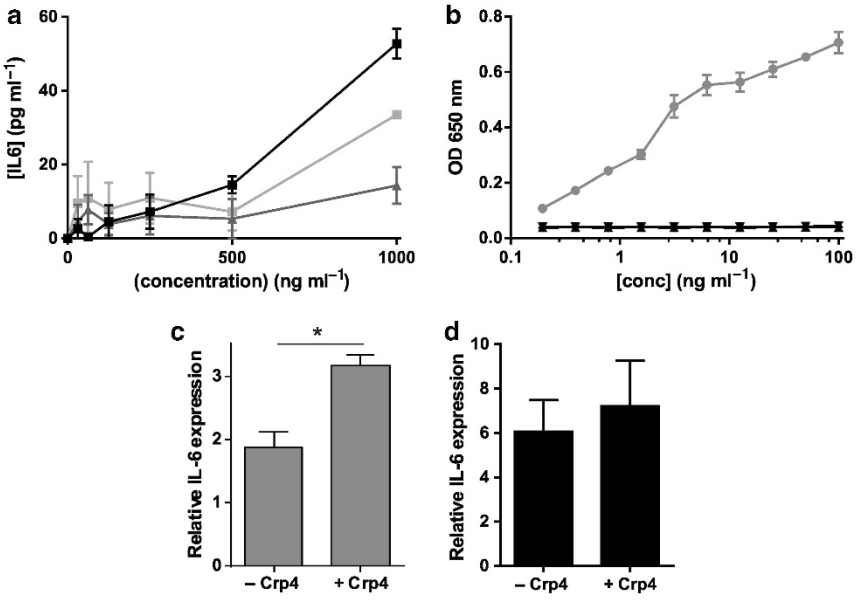

Figure 5 (**a**) IL-6 levels in the supernatant of thioglycollate-elicited macrophages incubated for 4 h with different increasing concentrations recombinant Crp1 (light gray), Crp3 (dark gray), and Crp4 (black). (**b**) $OD_{650\,nm}$ values of HEK-TLR4-Blue cells incubated for 24 h with increasing concentrations of recombinant Crp1, Crp3, and Crp4 (black). LPS (gray) was used as a positive control ($n=3$). (**c**,**d**) Relative IL-6 expression in ileum of MMP7$^{+/+}$ and MMP7$^{-/-}$ ileal explants incubated with and without Crp4 ($n=5$) (*$0.01 \leqslant P < 0.05$).

TLR4-dependent HEK-TLR4-Blue cell system (**Figure 5b**), we conclude that Crp1 and Crp4 induce inflammation in a TLR4-independent way and that the Crp preparation was free of LPS, as confirmed by specific LAL tests (data not shown). In addition, incubation of MMP7$^{-/-}$, but not MMP7$^{+/+}$, ileum explants with Crp4 resulted in an increase of IL-6 expression

(**Figure 5c,d**). These results indicate that cryptdins, next to having an important role in mucosal protection, also exhibit pro-inflammatory effects.

CONCLUSION

Intestinal permeability can eventually result in leakage of gut flora and/or damage-associated molecular patterns into the peripheral blood and tissues, and it is often believed that this has a central role in several inflammatory diseases.[45–47] In agreement with this and with previous results from our group,[48,49] we detected LPS-induced intestinal leakage of orally administered dextran and increased bacterial translocation to the MLNs. In addition, both EGF injection (which assures an optimal gut barrier function) and treatment with antibiotics (which removes all intestinal flora) resulted in protection against LPS-induced lethality and this was correlated with reduced intestinal permeability. These results show that loss of gut barrier integrity is an essential and detrimental process during LPS-induced systemic inflammation.

We demonstrate that MMP7 is upregulated during LPS-induced systemic in the Paneth cells and that MMP7-deficient mice are strongly protected against an otherwise lethal dose of LPS. Moreover, we show that this protease is essential in the propagation of gut leakage and consequent bacterial translocation to the MLNs. We propose that MMP7-activated cryptdins act as local amplifiers by stimulating the production of inflammatory mediators by inflammatory cells. Indeed, both Crp1 and Crp4 were able to induce TLR4-independent IL-6 production by macrophages. This further increases the local, intestinal inflammatory response, which is linked with increased inflammatory gene expression, intestinal damage, and a reduction in amount of mucin-containing goblet cells. Next, this results in increased gut permeability, bacterial efflux, subsequent multi-organ failure, and lethal shock. In contrast, all these processes were absent in MMP7-deficient mice, which are unable to produce active cryptdins in the small intestine. It is important to note that it was recently shown that α-defensins can be activated in the large bowel lumen, but not in the small intestine, of $MMP7^{-/-}$ mice by an MMP7-independent proteolytic mechanism.[50] However, the main portion of mature defensins is produced in the small intestine, so we believe that this alternative activation of defensins in $MMP7^{-/-}$ mice will only have a marginal effect and only in the large bowel. This pro-inflammatory role of the Paneth cells is in agreement with the results of a recent study by Park *et al.*[43], in which they showed that the Paneth cells initiate the cascade leading to multi-organ injury in response to acute kidney ischemia.

In conclusion, we show that MMP7 has detrimental effects in acute inflammation by amplifying the local intestinal inflammation. Our data suggest that this is due to the presence of pro-inflammatory, MMP7-activated cryptdins, but we do not rule out other MMP7 functions. Eventually, this phenomenon has an important role in LPS-induced loss of intestinal barrier integrity, bacterial translocation, multi-organ failure, and death. Although further research is needed, this pro-inflammatory effect of MMP7 may not only have a role in acute inflammation but also in chronic inflammation such as colitis, as colitis patients were shown to have increased MMP7 levels.[51–53]

METHODS

Animals. MMP7-deficient ($MMP7^{-/-}$) mice, which show no developmental abnormalities, were generated by gene targeting, as described previously.[17] All animals were backcrossed 12 times into a homogeneous C57BL6/J background. The C57BL/6J $MMP7^{+/+}$ and $MMP7^{-/-}$ mice were housed in an SPF animal facility with *ad libitum* access to food and water. Both male and female mice (8–12 weeks old) were used. All experiments were approved by the ethics committee of the Faculty of Science of Ghent University.

Injections, monitoring, and sampling of the mice. Mice were injected intraperitoneally with LPS from *Salmonella enterica serotype abortus equi* (Sigma, Diegem, Belgium) at 350 μg per 20 g body weight, the LD_{100} dose for wild-type C57BL/6 mice. In all experiments with sterile mice, LPS injections were performed intravenously to prevent injection into the swollen cecum. In this case, the LD_{100} dose for wild-type C57BL/6 mice is 250 μg per 20 g body weight. Recombinant mouse TNF was produced in *Escherichia coli* and purified to homogeneity in our laboratories with no detectable endotoxin contamination. Recombinant mouse TNF was diluted in PBS and injected intraperitoneally. The LD_{100} dose for wild-type C57BL/6 mice is 30 μg per 20 g body weight. Control animals received intraperitoneal or intravenous injections of PBS. EGF (E-4127; Sigma) was injected 0, 6, and 9 h after induction of endotoxemia (each time 2 μg per mouse). Rectal temperature was measured at different times after challenge. Blood and tissue samples were collected at designated times after injection. Mice were bled by heart puncture, and serum or EDTA plasma was prepared and stored at $-20\,^{\circ}C$ until use. For the explant experiments, mice were injected with an LD_{100} dose of LPS, the ileum was isolated 15 min later and incubated *ex vivo* in serum-free medium. To analyze DEFA5 levels, the supernatant was collected 1 h later. To study the effect of Crp4 on inflammatory gene expression, explants were incubated without and with Crp4 ($10\,\mu g\,ml^{-1}$) and RNA was isolated from the explants 4 h later.

Measurement of cytokines and DEFA5. Quantification of cytokines and chemokines in serum was performed using the Bio-Plex cytokine assays (Bio-Rad, Eke, Belgium), according to the manufacturer's instructions. HMGB1 (IBL International, Hamburg, Germany) and mouse DEFA5 (Uscn Life technologies, Huissen, The Netherlands) ELISAs were performed according to the manufacturer's instructions.

Lactate dehydrogenase and hexosaminidase activity. Lactate dehydrogenase activity in plasma was measured by the CytoTox 96 Assay (Promega, Leiden, The Netherlands) according the manufacturer's instructions. To determine the hexosaminidase activity, substrate solution (1 volume 7.5 mM p-nitrophenyl N-acetyl-β-D-glucosaminide (Sigma) in 0.1 M

sodium citrate pH 5 and 1 volume 0.5% Triton X100) was added to the plasma samples before incubation for 5 h at 37 °C. After adding the stop solution (100 nM glycine and 10 mM EDTA pH 10.4) absorbance is measured at 405 nm to determine relative hexosamidase activity.

Real time qPCR. Organs were stored in RNALater (Ambion, Ghent, Belgium) and RNA was isolated by using the RNeasy Mini Kit (Qiagen, Antwerp, Belgium). To enrich for the intestinal epithelial cell fraction in ileum samples, freshly isolated ileum samples were opened longitudinally, epithelial cells were scraped with a square glass coverslip and the scrapings were snap frozen. cDNA was synthesized by the iScript cDNA Synthesis Kit (Bio-Rad). Real-time PCR was performed on the LightCycler 480 system (Roche, Vilvoorde, Belgium) using the LightCycler 480 SYBR Green I Master (Roche). Expression levels were normalized to the expression of the two most stable housekeeping genes, which were determined for each organ using the geNorm Housekeeping Gene Selection Software (Biogazelle, Zwijnaarde, Belgium).[54] Primer sequences can be found in **Table 1**.

Histopathology and immunostaining of ileum sections. Tissues were fixed with PFA, embedded in paraffin and sectioned at 4 µm. For hematoxylin and eosin staining, sections were dewaxed and stained with hematoxylin (Fluka, Diegem, Belgium) and eosin (Merck, Leuven, Belgium). The degree of damage was evaluated on entire organ sections by three observers in a blinded manner. Intestinal damage is characterized by decreased villus height, epithelial cell death at the villus top and loss of mucus layer and goblet cells. Taking into account all histological features, a damage score ranging from 0 (normal) to 4 (abnormal) was given to each mouse. For alcian blue staining, sections were dewaxed and stained in alcian blue solution for 30 min, followed by two times 2 min washing in running tap water and distilled water. Sections were counterstained with nuclear fast red solution for 5 min, dehydrated, and mounted. For immunostaining, sections were dewaxed and boiled in 10 mM sodium citrate buffer for antigen retrieval, incubated for 1 h in blocking buffer (10 mM Tris-HCl pH 7.4, 0.1 M MgCl2, 0.5% Tween-20, 1% BSA, and 5% serum) and incubated with the antibodies of interest: LysC (1/50; sc-27958; Santa Cruz, Heidelberg, Germany), MMP7 (1/100; 3801; Cell Signaling Technology) and CD45 (1:250; 553078; Pharmingen). Fluorescent images and light microscopy images were taken by a laser scanning confocal microscope (Leica TCS SP5) and an Olympus light microscope, respectively.

Table 1 Overview qPCR primers

Gene name	Forward primer	Reversed primer
Mmp7	ACTTCAGACTTACCTCGGATCG	TCCCCCAACTAACCCTCTTGA
Defcr1	CAGGCCGTATCTGTCTCCTT	ATGACCCTTTCTGCAGGTTC
Defcr3	CCCAGAAGGCTCTTCTCTTC	CAGCGACAGCAGAGTGTGTA
RegIIIγ	TTCCTGTCCTCCATGATCAAAA	CATCCACCTCTGTTGGGTTCA
IL-6	TAGTCCTTCCTACCCCAATTTCC	TTGGTCCTTAGCCACTCCTTC
TNF	ACCCTGGTATGAGCCCATATAC	ACACCCATTCCCTTCACAGAG
iNOS	TGGTCCGCAAGAGAGTGCT	CCTCATTGGCCAGCTGCTT
Rpl	CCTGCTGCTCTCAAGGTT	TGGCTGTCACTGCCTGGTACTT
Ubc	AGGTCAAACAGGAAGACAGACGTA	TCACACCCAAGAACAAGCACA
Gapdh	TGAAGCAGGCATCTGAGGG	CGAAGGTGGAAGAGTGGGAG
Hprt	AGTGTTGGATACAGGCCAGAC	CGTGATTCAAATCCCTGAAGT
Hmbs	GAAACTCTGCTTCGCTGCATT	TGCCCATCTTTCATCGTATG

Toluidin blue staining. One percentage gluteraldehyde-fixed semithin sections were stained with toluidine blue. The amount of toluidine blue-positive granules per crypt was counted automatically by using the Volocity software (PerkinElmer, Zaventem, Belgium).

Western blot analysis. The ileum samples were isolated, flushed with ice-cold PBS and homogenized in 1% NP40 lysis buffer. Protein concentration was determined by BCA assay (Pierce, Erembodegem, Belgium) and samples were analyzed by western blot. Blots were incubated overnight with anti-actin (1/10000; 691002, MP Biomedicals, Brussels, Belgium) and anti-MMP7 (1/200; 3801, Cell Signaling Technology). Immunoreactive proteins were visualized and quantified using the Odyssey Infrared Imaging System and Odyssey software as described by the manufacturer (Li-Cor).

Gut permeability. FITC-labeled dextran (4 kDa, Sigma) was administered to mice by gavage at 150 mg per kg body weight. Five hours later, blood was obtained by heart puncture, collected in EDTA-coated tubes (Sarstedt, Hoogstraten, Belgium) and plasma was prepared. Leakage of FITC-labeled dextran into the circulation was determined by measurement of the plasma fluorescence ($\lambda_{ex}/\lambda_{em} = 488/520$ nm). Values were normalized to the lowest value.

Bacterial counts in MLN. Before and after LPS injection, MLNs were isolated, homogenized in 200 µl brain heart infusion medium (Becton Dickinson, Erembodegem, Belgium), plated onto tryptic soy agar plates, and incubated at 37 °C. The following day, the number of colony forming units per ml was determined.

Depletion of commensal intestinal bacteria. To eliminate commensal bacteria, their drinking water was supplemented with 200 mg l^{-1} ciprofloxacin (Sigma-Aldrich, Diegem, Belgium), 1 g l^{-1} ampicillin (Sigma-Aldrich), 1 g l^{-1} metronidazole (Sigma-Aldrich), and 500 mg l^{-1} vancomycin (Labconsult). After 2 weeks, the presence of colonic microflora was determined by culturing fecal samples in brain heart infusion and in thioglycollate medium (Sigma-Aldrich).

Thioglycollate macrophages. Mice were injected intrperitoneally with 2 ml 3% thioglycollate and 4 days later thioglycollate-elicited macrophages were isolated by peritoneal lavage with ice-cold PBS. Cells were counted and seeded at 2×10^6 cells per six-well plate in LPS-free DMEM supplemented with 10% FCS and penicillin–streptomycin. Four hours later, the medium was replaced with fresh medium containing different

concentrations recombinant cryptdins. Crp1, -3, and -4 were a kind gift from Professor Andre Ouelette (Los Angeles).

HEK-TLR4-blue cells. HEK-TLR4-Blue TLR cells (Invivogen, Toulouse, France) that stably co-express the TLR4 gene and an NF-κB-inducible SEAP (secreted embryonic alkaline phosphatase) reporter gene were incubated with increasing concentrations of Crp1, Crp3, and Crp4. SEAP activity was monitored with QUANTI-Blue according to manufacturer's instructions.

Statistical analysis. Data are presented as means ± s.e. of mean. Data were analyzed with an unpaired Mann–Whitney U-test, unless mentioned differently. Survival curves were compared using a log-rank test. Significance levels were calculated for differences from the corresponding 0 h time point and/or between $MMP7^{+/+}$ and $MMP7^{-/-}$ mice, as indicated ($^{*}0.01 \leq P < 0.05$; $^{**}0.001 \leq P < 0.01$; $^{***}P < 0.001$).

SUPPLEMENTARY MATERIAL is linked to the online version of the paper at http://www.nature.com/mi

ACKNOWLEDGMENTS

This work was supported by the Research Council of Ghent University, the Research Foundation Flanders (FWO Vlaanderen), and the Interuniversity Attraction Poles Program of the Belgian Science Policy. We would like to thank Joke Vanden Berghe, Kelly Lemeire and the DMBR Microscopy Core for technical assistance and Amin Bredan for editing the manuscript.

REFERENCES

1. Williams, SC. After Xigris, researchers look to new targets to combat sepsis. *Nat. Med.* **18**, 1001 (2012).
2. Shen, L & Turner, JR. Role of epithelial cells in initiation and propagation of intestinal inflammation. Eliminating the static: tight junction dynamics exposed. *Am. J. Physiol. Gastrointest. Liver Physiol.* **290**, G577–G582 (2006).
3. Macintire, DK & Bellhorn, TL. Bacterial translocation: clinical implications and prevention. *Vet. Clin. North Am. Small Anim. Pract.* **32**, 1165–1178 (2002).
4. Gatt, M, Reddy, BS & MacFie, J. Review article: bacterial translocation in the critically ill–evidence and methods of prevention. *Aliment. Pharmacol. Ther.* **25**, 741–757 (2007).
5. Li, Q, Zhang, Q, Wang, C, Liu, X, Li, N & Li, J. Disruption of tight junctions during polymicrobial sepsis *in vivo*. *J. Pathol.* **218**, 210–221 (2009).
6. Puleo, F, Arvanitakis, M, Van Gossum, A & Preiser, JC. Gut failure in the ICU. *Semin. Respir. Crit. Care Med.* **32**, 626–638 (2011).
7. Papoff, P. *et al.* Gut microbial translocation in critically ill children and effects of supplementation with pre- and pro biotics. *Int. J. Microbiol.* **2012**, 151393 (2012).
8. Vandenbroucke, RE. *et al.* Matrix metalloproteinase 13 modulates intestinal epithelial barrier integrity in inflammatory diseases by activating TNF. *EMBO Mol. Med.* **5**, 932–948 (2013).
9. Ayabe, T, Satchell, DP, Wilson, CL, Parks, WC, Selsted, ME & Ouellette, AJ. Secretion of microbicidal alpha-defensins by intestinal Paneth cells in response to bacteria. *Nat. Immunol.* **1**, 113–118 (2000).
10. Andersson, ML, Karlsson-Sjoberg, JM & Putsep, KL. CRS-peptides: unique defense peptides of mouse Paneth cells. *Mucosal Immunol.* **5**, 367–376 (2012).
11. Hornef, MW, Putsep, K, Karlsson, J, Refai, E & Andersson, M. Increased diversity of intestinal antimicrobial peptides by covalent dimer formation. *Nat. Immunol.* **5**, 836–843 (2004).
12. Ouellette, AJ & Bevins, CL. Paneth cell defensins and innate immunity of the small bowel. *Inflamm. Bowel Dis.* **7**, 43–50 (2001).
13. Vanlaere, I & Libert, C. Matrix metalloproteinases as drug targets in infections caused by gram-negative bacteria and in septic shock. *Clin. Microbiol. Rev.* **22**, 224–239 (2009).
14. Vandenbroucke, RE, Dejonckheere, E & Libert, C. A therapeutic role for matrix metalloproteinase inhibitors in lung diseases?. *Eur. Respir. J.* **38**, 1200–1214 (2011).
15. Dejonckheere, E, Vandenbroucke, RE & Libert, C. Matrix metalloproteinases as drug targets in ischemia/reperfusion injury. *Drug Discov. Today* **16**, 762–778 (2011).
16. Vandenbroucke, RE. *et al.* Matrix Metalloprotease 8-Dependent Extracellular Matrix Cleavage at the Blood-CSF Barrier Contributes to Lethality during Systemic Inflammatory Diseases. *J. Neurosci.* **32**, 9805–9816 (2012).
17. Wilson, CL. *et al.* Regulation of intestinal alpha-defensin activation by the metalloproteinase matrilysin in innate host defense. *Science* **286**, 113–117 (1999).
18. Pal, S, Schmidt, AP, Peterson, EM, Wilson, CL & de la Maza, LM. Role of matrix metalloproteinase-7 in the modulation of a Chlamydia trachomatis infection. *Immunology* **117**, 213–219 (2006).
19. Swee, M, Wilson, CL, Wang, Y, McGuire, JK & Parks, WC. Matrix metalloproteinase-7 (matrilysin) controls neutrophil egress by generating chemokine gradients. *J. Leukoc. Biol.* **83**, 1404–1412 (2008).
20. Zuo, F. *et al.* Gene expression analysis reveals matrilysin as a key regulator of pulmonary fibrosis in mice and humans. *Proc. Natl. Acad. Sci. USA* **99**, 6292–6297 (2002).
21. Shi, J. *et al.* A novel role for defensins in intestinal homeostasis: regulation of IL-1beta secretion. *J. Immunol.* **179**, 1245–1253 (2007).
22. Cantaluppi, V. *et al.* Polymyxin-B hemoperfusion inactivates circulating proapoptotic factors. *Intensive Care Med.* **34**, 1638–1645 (2008).
23. Cruz, DN. *et al.* Early use of polymyxin B hemoperfusion in abdominal septic shock: the EUPHAS randomized controlled trial. *JAMA* **301**, 2445–2452 (2009).
24. Cruz, DN. *et al.* Effectiveness of polymyxin B-immobilized fiber column in sepsis: a systematic review. *Crit. Care* **11**, R47 (2007).
25. Wang, H, Zhu, S, Zhou, R, Li, W & Sama, AE. Therapeutic potential of HMGB1-targeting agents in sepsis. *Expert Rev. Mol. Med.* **10**, e32 (2008).
26. Tucker, SM & Price, RG. Changes in human hexosaminidase isoenzyme distribution in body fluids during the course of tissue damage. *Biochem. Soc. Trans.* **5**, 241–243 (1977).
27. Ayabe, T. *et al.* Activation of Paneth cell alpha-defensins in mouse small intestine. *J. Biol. Chem.* **277**, 5219–5228 (2002).
28. Rumio, C. *et al.* Induction of Paneth cell degranulation by orally administered Toll-like receptor ligands. *J. Cell Physiol.* **227**, 1107–1113 (2012).
29. Lopez-Boado, YS, Wilson, CL, Hooper, LV, Gordon, JI, Hultgren, SJ & Parks, WC. Bacterial exposure induces and activates matrilysin in mucosal epithelial cells. *J. Cell Biol.* **148**, 1305–1315 (2000).
30. Berlanga, J. *et al.* Prophylactic use of epidermal growth factor reduces ischemia/reperfusion intestinal damage. *Am. J. Pathol.* **161**, 373–379 (2002).
31. Berlanga, J, Lodos, J & Lopez-Saura, P. Attenuation of internal organ damages by exogenously administered epidermal growth factor (EGF) in burned rodents. *Burns* **28**, 435–442 (2002).
32. Liu, Q, Djuricin, G, Nathan, C, Gattuso, P, Weinstein, RA & Prinz, RA. The effect of epidermal growth factor on the septic complications of acute pancreatitis. *J. Surg. Res.* **69**, 171–177 (1997).
33. Clark, JA, Gan, H, Samocha, AJ, Fox, AC, Buchman, TG & Coopersmith, CM. Enterocyte-specific epidermal growth factor prevents barrier dysfunction and improves mortality in murine peritonitis. *Am. J. Physiol. Gastrointest. Liver Physiol.* **297**, G471–G479 (2009).
34. Clark, JA, Clark, AT, Hotchkiss, RS, Buchman, TG & Coopersmith, CM. Epidermal growth factor treatment decreases mortality and is associated with improved gut integrity in sepsis. *Shock* **30**, 36–42 (2008).
35. Dominguez, JA. *et al.* Epidermal growth factor improves survival and prevents intestinal injury in a murine model of pseudomonas aeruginosa pneumonia. *Shock* **36**, 381–389 (2011).
36. Dvorak, B. *et al.* Epidermal growth factor reduces the development of necrotizing enterocolitis in a neonatal rat model. *Am. J. Physiol. Gastrointest. Liver Physiol.* **282**, G156–G164 (2002).

37. Fink, MP. Intestinal epithelial hyperpermeability: update on the pathogenesis of gut mucosal barrier dysfunction in critical illness. *Curr. Opin. Crit. Care* **9**, 143–151 (2003).
38. Salzman, NH. *et al.* Enteric defensins are essential regulators of intestinal microbial ecology. *Nat Immunol* **11**, 76–83 (2010).
39. Turner, JR. Intestinal mucosal barrier function in health and disease. *Nat. Rev. Immunol.* **9**, 799–809 (2009).
40. John, LJ, Fromm, M & Schulzke, JD. Epithelial barriers in intestinal inflammation. *Antioxid. Redox Signal* **15**, 1255–1270 (2011).
41. Noth, R. *et al.* Anti-TNF-alpha antibodies improve intestinal barrier function in Crohn's disease. *J. Crohns Colitis* **6**, 464–469 (2012).
42. Marchiando, AM. *et al.* Caveolin-1-dependent occludin endocytosis is required for TNF-induced tight junction regulation *in vivo*. *J. Cell Biol.* **189**, 111–126 (2010).
43. Park, SW. *et al.* Paneth cell-mediated multiorgan dysfunction after acute kidney injury. *J. Immunol.* **189**, 5421–5433 (2012).
44. Takahashi, N. *et al.* IL-17 produced by Paneth cells drives TNF-induced shock. *J. Exp. Med.* **205**, 1755–1761 (2008).
45. Ilan, Y. Leaky gut and the liver: a role for bacterial translocation in non-alcoholic steatohepatitis. *World J. Gastroenterol.* **18**, 2609–2618 (2012).
46. Faries, PL, Simon, RJ, Martella, AT, Lee, MJ & Machiedo, GW. Intestinal permeability correlates with severity of injury in trauma patients. *J. Trauma* **44**, 1031–1035 (1998).
47. Swank, GM & Deitch, EA. Role of the gut in multiple organ failure: bacterial translocation and permeability changes. *World J. Surg.* **20**, 411–417 (1996).
48. Vandenbroucke, RE. *et al.* Matrix metalloproteinase 13 modulates intestinal epithelial barrier integrity in inflammatory diseases by activating TNF. *EMBO Mol. Med.* **5**, 1000–1016 (2013).
49. Van Hauwermeiren, F. *et al.* Safe TNF-based antitumor therapy following p55TNFR reduction in intestinal epithelium. *J. Clin. Invest.* **123**, 2590–2603 (2013).
50. Mastroianni, JR, Costales, JK, Zaksheske, J, Selsted, ME, Salzman, NH & Ouellette, AJ. Alternative luminal activation mechanisms for paneth cell alpha-defensins. *J. Biol. Chem.* **287**, 11205–11212 (2012).
51. Noble, CL. *et al.* Regional variation in gene expression in the healthy colon is dysregulated in ulcerative colitis. *Gut* **57**, 1398–1405 (2008).
52. Rath, T. *et al.* Enhanced expression of MMP-7 and MMP-13 in inflammatory bowel disease: a precancerous potential? *Inflamm. Bowel Dis.* **12**, 1025–1035 (2006).
53. Rath, T, Roderfeld, M, Halwe, JM, Tschuschner, A, Roeb, E & Graf, J. Cellular sources of MMP-7, MMP-13 and MMP-28 in ulcerative colitis. *Scand. J. Gastroenterol.* **45**, 1186–1196 (2010).
54. Vandesompele, J. *et al.* Accurate normalization of real-time quantitative RT-PCR data by geometric averaging of multiple internal control genes. *Genome Biol.* **3**, RESEARCH0034 (2002).